

## Improved energy storage performance of sandwich-structured P(VDF-HFP)-based nanocomposites by the additions of inorganic nanoparticles

Yan Guo,<sup>a</sup> Di Zhou,<sup>\*a</sup> Da Li,<sup>a</sup> Weichen Zhao,<sup>a</sup> Yifei Wang,<sup>b</sup> Lixia Pang,<sup>c</sup> Zhongqi Shi,<sup>d</sup>  
Tao Zhou,<sup>e</sup> Shikuan Sun,<sup>f</sup> Charanjeet Singh,<sup>g</sup> Sergei Trukhanov,<sup>h</sup> Antonio Sergio  
Bezerra Sombra,<sup>i</sup> and Guohua Chen<sup>j</sup>

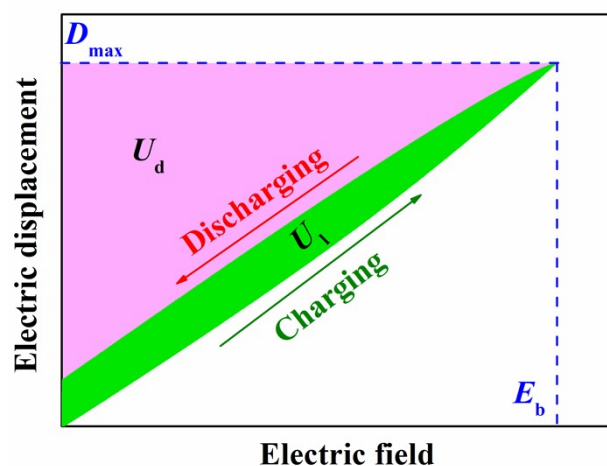


Fig.S1. Schematic diagram of hysteresis loop of nonlinear dielectric.

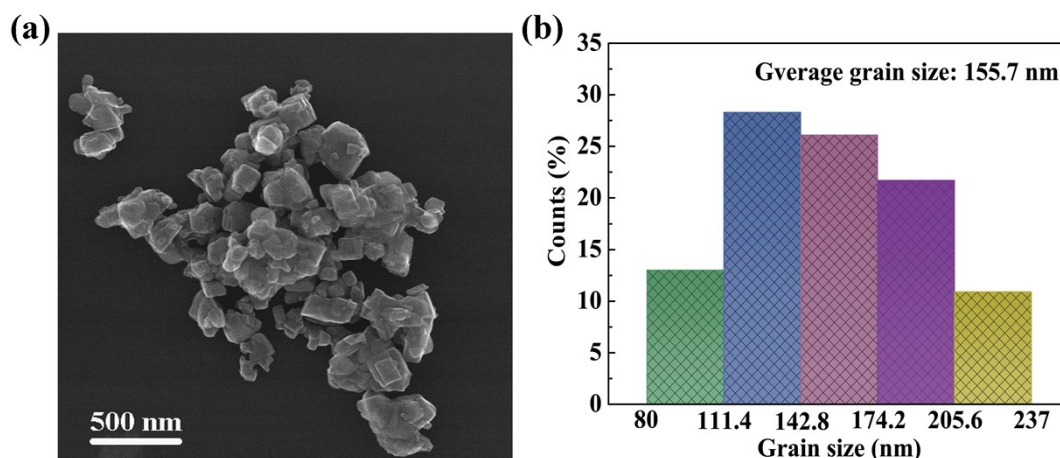
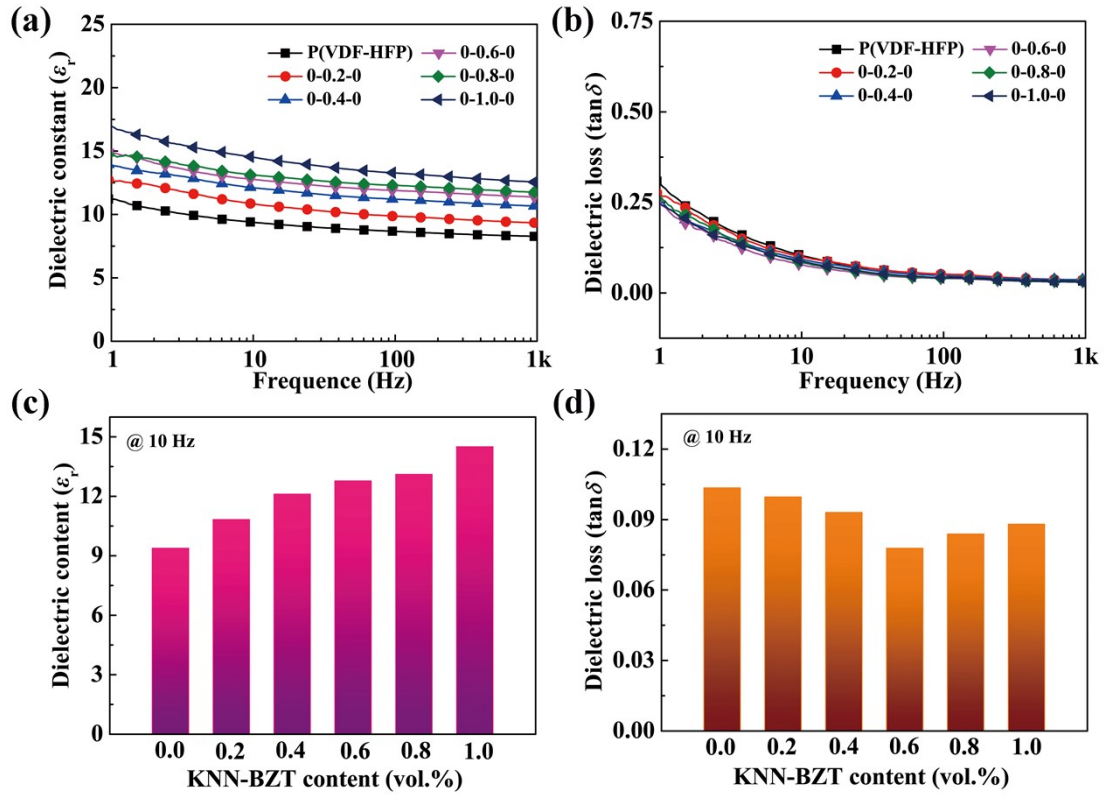
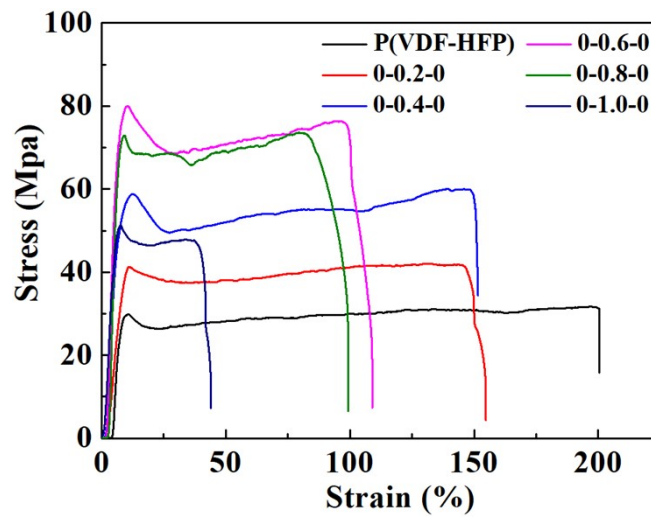


Fig.S2. TEM image (a) and grain size distribution (b) of KNN-BZT nanoparticles.

\*Corresponding author E-mail address: zhoudi1220@gmail.com (Di Zhou)



**Fig.S3.** (a) and (b) Dielectric properties of sandwich-structured nanocomposites at 1 Hz-1 kHz. (c) and (d) are the dielectric constants and losses of nanocomposites at 10 Hz.



**Fig.S4.** Stress-strain curves of sandwich-structured nanocomposites.

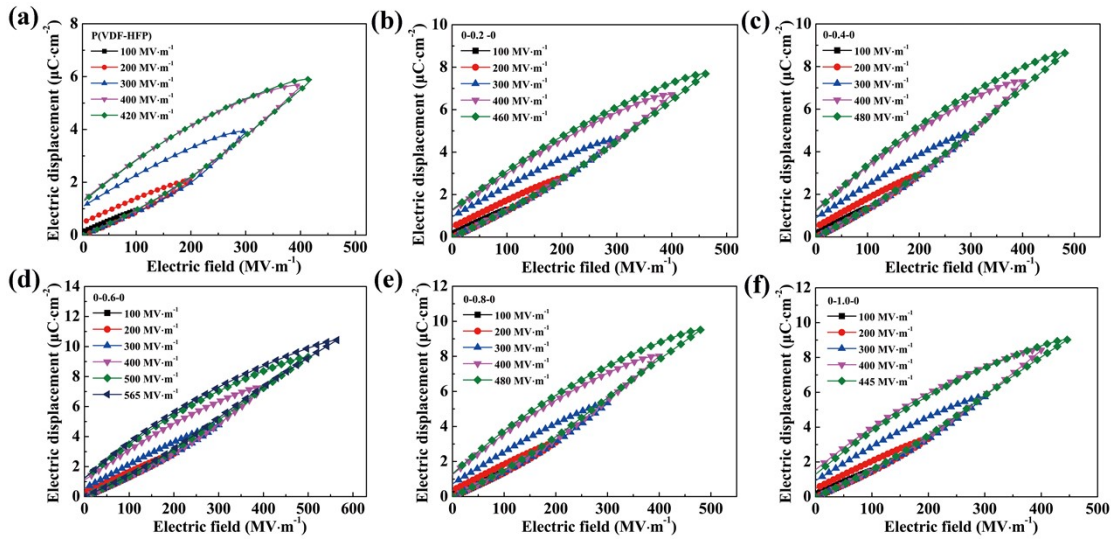


**Fig.S5.** Hysteresis loops of sandwich-structured nanocomposites under different electric fields.

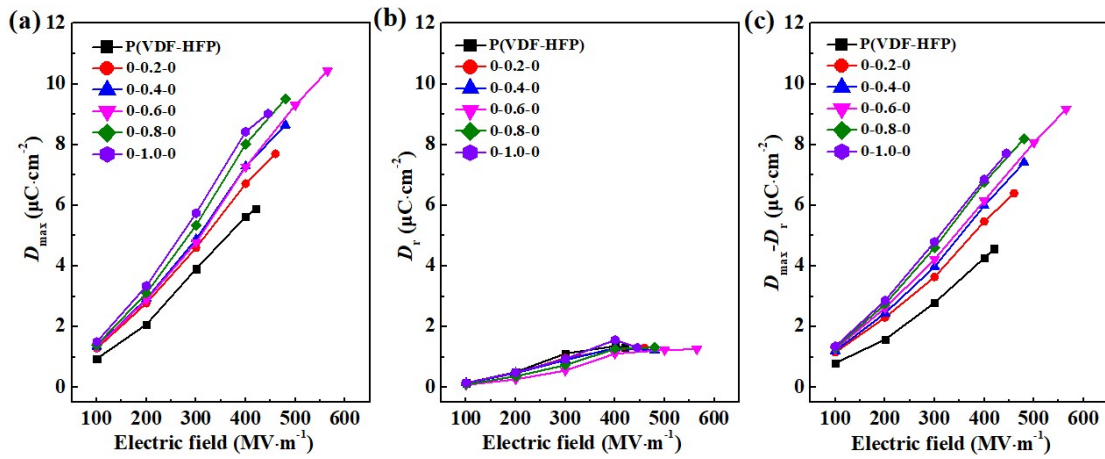


**Fig.S6.**  $D_{\max}$ ,  $D_r$  and  $D_{\max} - D_r$  of sandwich-structured nanocomposites under different electric fields.

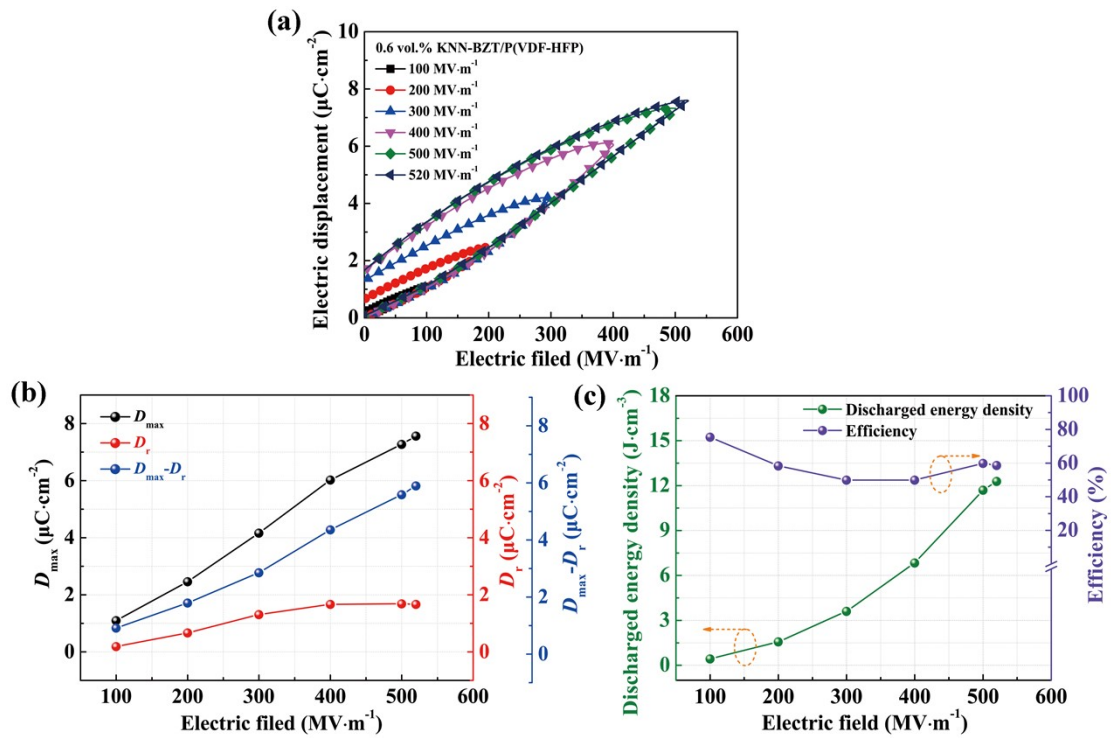


**Fig.S7.** Single-layer 0.6 vol.% KNN-BZT/P(VDF-HFP) nanocomposites: (a) Hysteresis loops; (b)  $D_{\text{max}}$ ,  $D_{\text{r}}$  and  $D_{\text{max}} - D_{\text{r}}$ ; (c) Discharged energy density and efficiency.